

## Research on the Output Characteristics of Photovoltaic Array under the Non-Uniform Light

Zhang Junhong Wei Xueye and Zhu Tianlong

*School of Electronic and Information Engineering, Beijing Jiaotong University, China, 100044*

*School of Electrical and information Engineering, Beijing University of Civil Engineering and Architecture, China, 100044*

### Abstract

*The output characteristics of photovoltaic array was related with the topology of array, shadow distribution and illumination level. The theoretical analysis and simulation modeling of output characteristics of photovoltaic array including series array, parallel array and series-parallel array were made under the non-uniform illumination environment based on the circuit analysis. The photovoltaic cell was modeled by use of the improved two-diode model. Non uniform illumination is expanded from two illumination levels of traditional to N illumination levels and from the single series array to any number series-parallel array. The different analysis methods were adopted in different arrays for mathematical modeling and simulation. The current analysis was used in series arrays and voltage analysis used in parallel arrays. Analysis of current in branches and voltage between branches was used in series-parallel array. Then the mathematical models were established and programmed in m-file by MATLAB. The simulation models had a high computational accuracy, and were suitable for any simulation output characteristics of PV in different light environment and array topology. They could provide a theoretical basis for constructing the topological structure on the same condition and studying MPPT of PV array under non-uniform illumination.*

**Keywords:** *PV array; Non-uniform illumination; Circuit analysis; Output characteristics*

### 1. Introduction

Photovoltaic (PV) array as the energy supply unit of a photovoltaic system, research on the output characteristics of photovoltaic array had important significance for array optimal allocation and the Maximum Power Point Tracking (MPPT). The output characteristics of PV modules and photovoltaic arrays remain consistent, showing a single peak characteristic under uniform illumination [1-3]. However, with more and more extensive application of photovoltaic power generation, the environment had become more complex. The local shadow problem was difficult to avoid especially the installation of PV systems in the densely built area. It resulted in the output power of PV array showing multi-peak characteristics, which increased the difficulty of MPPT to control and seriously affected the efficiency of photovoltaic power generation system. It had a great practical significance for modeling and the output characteristics for non-uniform conditions of photovoltaic array.

Many scholars had done a theoretical and experimental study for a long time. In literatures [4-7], the single module or the two series modules under local shadows was discussed without considering the large photovoltaic arrays. The engineering mathematical model was analyzed in the literatures [8-9], although the model was

simple in calculation, the precision was poor. The improved single and double diode models were adopted to describe the circuit of PV array respectively in literatures [10-13], which had high accuracy and fast simulation speed. The characteristic of different sub-array in different shading levels was modeled and analyzed in literature [14], but the sub-array was not considered in a non-uniform illumination conditions. Although the literatures [15-17] discussed the output characteristic curve of PV array by MATLAB simulation with one shadow level, but it avoided the modeling under complex shading conditions.

Taking the series-parallel photovoltaic array as the research object, the output models were deduced under non-uniform illumination based on the circuit analysis in this paper. A series of conclusions were concluded about the series array, parallel array and series-parallel array.

## 2. PV Array Modeling

PV array was composed of photovoltaic modules by some series and parallels, and PV module was composed of some photovoltaic cells series.

### 2.1. PV Cell Model of Double Diode

The double-diode PV cell model was shown in Figure 1.

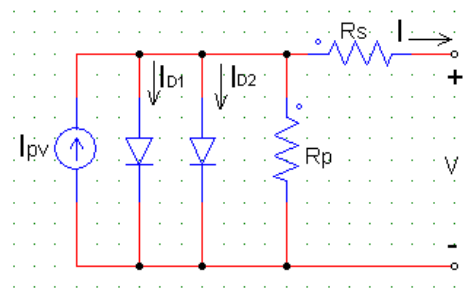


**Figure 1. PV Cell Model of Double-Diode**

$I$ ,  $V$  expressed respectively for output voltage and current of PV cell, which:

$$I = I_{pv} - I_{D1} - I_{D2} - \frac{V + R_s I}{R_p} \quad (1)$$

$I_{pv}$ : photocurrent;  $R_s$ ,  $R_p$ : parallel and series equivalent resistance of the cell.

$$I_{D1} = I_{01} \left[ \exp\left(\frac{V + R_s I}{V_{T1}}\right) - 1 \right]$$

$$I_{D2} = I_{02} \left[ \exp\left(\frac{V + R_s I}{V_{T2}}\right) - 1 \right]$$

$V_{T1} = A_1 KT/q$ ,  $V_{T2} = A_2 KT/q$ ,  $V_{T1}$ ,  $V_{T2}$ : thermal voltage of the cell;

$A_1, A_2$ : diode D1 and D2 ideality factor;

$Q$ : unit charge,  $1.6022 \times 10^{-19} C$ ;

$K$ : Pohl Weitzman constant,  $1.3806 \times 10^{-22} J / K$ ;

$I_{01}$ ,  $I_{02}$ : Diode D1, D2 reverse saturation current;

$T$ : The absolute temperature of PV cell, K.

The output current expression of PV cell:

$$I = I_{pv} - I_{01}[\exp(\frac{V + R_s I}{V_{T1}}) - 1] - I_{02}[\exp(\frac{V + R_s I}{V_{T2}}) - 1] - \frac{V + R_s I}{R_p} \quad (2)$$

## 2.2. The Mathematical Model of PV Module

The current expression of the PV module composed of  $N_s$  PV cells in series was:

$$I = I_{pv} - I_{01}[\exp(\frac{V + R_{Ms} I}{N_s V_{T1}}) - 1] - I_{02}[\exp(\frac{V + R_{Ms} I}{N_s V_{T2}}) - 1] - \frac{V + R_{Ms} I}{R_{Mp}} \quad (3)$$

$R_{Ms} = R_s N_s$ ,  $R_{Mp} = R_p N_s$ , series and shunt resistance of PV module

Parameters in formula (3) are calculated based on the improved diode model [11,13].

$$I_{pvn} = \frac{(R_{Ms} + R_{Mp}) I_{scn}}{R_{Mp}} \quad I_{pv} = (I_{pvn} + K_i \Delta T) \frac{G}{G_n}$$

$$I_{01} = I_{02} = \frac{I_{scn} + K_i \Delta T}{\exp[(V_{ocn} + K_v \Delta T) / V_T] - 1}$$

$$A_1=1, A_2=2$$

$V_{ocn}$ ,  $I_{scn}$ : open circuit voltage and short circuit current under standard conditions;

$\Delta T = T - T_s$ ,  $T_s$ : standard temperature, 250C;

G: illumination standard;

$G_n$ : standard temperature, 1000W/m<sup>2</sup>;

Electrical characteristics parameters of KG200GT cell was shown in Table 1.

**Table 1. Electrical Parameters of KG200GT**

Parameters	Value
Cell structure	Ns=54
Maximum power $P_m$	270W
open circuit voltage Voc	32.9V
maximum power point voltage Vm	26.3.7 V
maximum power point current Im	7.63A
Short circuit current Isc	8.21A
Voltage / temperature coefficient Kv	-0.36%/°C
Current / temperature coefficient Ki	0.060%/°C

**Table 2. Electrical Parameters for Improved Double-Diode Model**

Parameters	Value
Cell structure	Ns=54
Maximum power Pm	270W
The maximum power point voltage Vm	26.3V
The maximum power point current Im	7.63A
Reverse saturation current IO	$4.128 \times 10^{-10}$ A
Photocurrent Ipv	8.22 A
Series resistance Rs	0.335Ω
Parallel resistance Rp	155.48Ω

### 2.3. The Mathematical Model of PV Array

Mathematical model of Nsa modules in serials:

$$I = I_{pv} - I_{01} \left[ \exp\left(\frac{V + R_{Ms} I N_{sa}}{N_s V_{T1} N_{sa}}\right) - 1 \right] - I_{02} \left[ \exp\left(\frac{V + R_{Ms} I N_{sa}}{N_s N_{sa} V_{T2}}\right) - 1 \right] - \frac{V + R_{Ms} I N_{sa}}{N_{sa} R_{Mp}} \quad (4)$$

Mathematical model of Npa modules in parallels:

$$I = I_{pv} - I_{01} \left[ \exp\left(\frac{V + R_{Ms} I / N_{pa}}{N_s V_{T1} / N_{pa}}\right) - 1 \right] - I_{02} \left[ \exp\left(\frac{V + R_{Ms} I / N_{pa}}{N_s V_{T2} / N_{pa}}\right) - 1 \right] - \frac{V + R_{Ms} I / N_{pa}}{R_{Mp} / N_{pa}} \quad (5)$$

Mathematical model of Nsa and Npa modules in series and parallels:

$$I = I_{pv} - I_{01} \left[ \exp\left(\frac{V + R_{Ms} I (N_{sa} / N_{pa})}{N_s V_{T1}}\right) - 1 \right] - I_{02} \left[ \exp\left(\frac{V + R_{Ms} I (N_{sa} / N_{pa})}{N_s V_{T2}}\right) - 1 \right] - \frac{V + R_{Ms} I (N_{sa} / N_{pa})}{R_{Mp} (N_{sa} / N_{pa})} \quad (6)$$

## 3. PV Array Mathematical Models under Non-uniform Illumination

### 3.1. The Mathematical Model of PV Series Arrays

The light intensity of series modules was not all the same under non-uniform illumination, which produced different optical current and output voltage. Some bypass diodes connected with modules in parallel were in conducting state for forward bias, which change the output characteristics of series array.

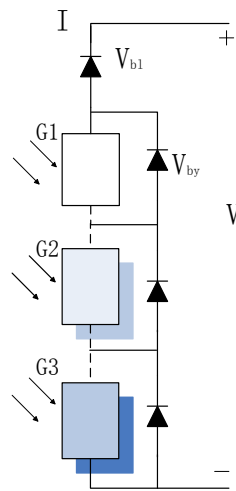


Figure 2. Series PV Array

In Figure 2, Series array consisted of N modules, N1 modules for illumination G1, i.e.  $N_1(G1)$ ,  $N_2(G2)$ ,  $N_3(G3)$ ,  $G1 > G2 > G3$ ,  $N = N_1 + N_2 + N_3$ . The photocurrent of these modules were respectively  $I_{pv1}$ ,  $I_{pv2}$ ,  $I_{pv3}$  and the corresponding to short circuit current  $I_{cs1}$ ,  $I_{cs2}$ ,  $I_{cs3}$ , output voltage  $V_{N1}$ ,  $V_{N2}$ ,  $V_{N3}$ .

The output current is divided into three independent intervals reference for the current. The object of study was turned from series array to independent modules to simplify the analysis object. It had the following steps:

(1) N modules output power

As the output current  $I \in [0, I_{cs3}]$ , the current  $I$  was generated by the illumination of G3 modules and all the bypass diodes were in the blocking state for reverse bias. The output voltages were the sum of  $V_{N_1}$ ,  $V_{N_2}$  and  $V_{N_3}$ , corresponding to G1, G2 and G3 modules.

$$V = V_{N_1} + V_{N_2} + V_{N_3} + V_{bl}$$

$V_{bl}$ : the conducted voltage of series blocking diode.

The  $N_1$ ,  $N_2$  and  $N_3$  into the formula (4), then

$$V_{N_i} = N_i R_{Mp} \left\{ I_{pvi} - I_{01} \left[ \exp\left(\frac{V_{N_i} + R_{Ms} I N_i}{N_s V_{T1} N_i}\right) - 1 \right] - I_{02} \left[ \exp\left(\frac{V_{N_i} + R_{Ms} I N_i}{N_s N_i V_{T2}}\right) - 1 \right] - I \right\} - R_{Ms} I N_i \quad (i=1,2,3)$$

$$V_{bl} = \frac{AKT}{q} \ln\left(\frac{I}{I_0} + 1\right) \quad (7)$$

$I_0$ : Reverse saturation current,  $0.15 \times 10^{-6}$  A;

A: Ideality factor, 1.75.

(2) N1 and N2 modules output power

When the output current  $I \in [I_{cs3}, I_{cs2}]$ , the bypass diodes parallel with  $N_3$  modules were conducted for a forward bias voltage. The current  $I - I_{pv3}$  flowed through the G3 modules exported by the bypass diodes. The output voltage equation was as following:

$$V = V_{N_1} + V_{N_2} + N_3 V_{by} + V_{bl} \quad (8)$$

$V_{by}$ : voltage of diodes parallel with G3 modules as it conducted.

$$V_{by} = \frac{AKT}{q} \ln\left(\frac{I}{I_0} + 1\right) \quad (9)$$

(3)  $N_1$  modules output power

When the output current  $I \in (I_{cs3}, I_{cs2}]$ , the bypass diodes parallel with G2 and G3 modules were conducted. The current  $I$  was provided by G1 modules.

$$V = V_{N_1} + N_2 V_{by} + N_3 V_{by} + V_{bl} \quad (10)$$

The output characteristics of series array were consistent to  $N_1$  (G1), only lagging ( $N_2+N_3$ ) voltages drop of bypass diodes in voltage distribution. It had a peak power, but not necessarily the global MPP.

With the array output current decreasing, the output voltage and power of G1 modules increased slowly. When the current decreased to  $[I_{cs3}, I_{cs2}]$ , the output power of G2 modules increased gradually until MPP. When the output current decreased to  $[0, I_{cs3}]$ , the power of G3 modules increased gradually, then the power reached another peak point. The output characteristics of series array showed the single peak characteristics of G2 and G3 modules in the trend and value addition of all the work modules in the numerical.

To sum up, it had three peak power points in the output current range for the three levels G1, G2 and G3 in non-uniform illumination and could be extended to  $M$  levels with  $M$  peak power points and expressed by piecewise function forms.

### 3.2. The Mathematical Model of Parallel PV Arrays

The parallel array was composed of parallel modules, the topology shown in Figure 3. In the non-uniform illumination, the modules generated different optical currents and output voltages, which changed the output characteristic because the blocking diodes ( $V_{b1}$ ) serial with branch modules could be reversed. The output voltage was divided into three independent intervals as reference for the output voltage. The research object was turned from the parallel arrays to independent modules as the current in each branch calculated in order to simplify the analysis object.

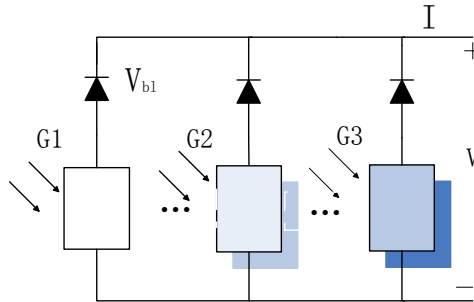


Figure 3. Parallel PV Array

In Figure 3  $N_1$  ( $G_1$ ),  $N_2$  ( $G_2$ ),  $N_3$  ( $G_3$ ) corresponding to the open circuit voltages were  $V_{oc1} > V_{oc2} > V_{oc3}$ . The output process could be divided into three sections:

(1)  $N$  modules output power

As the output voltage of parallel array  $V \in [0, V_{oc3}]$ , all the modules worked at the same voltage together. The blocking diodes were forward conduction, at the same time, output current  $I$  of array was the sum of all the parallel branches.

$$I = I_{N_1} + I_{N_2} + I_{N_3} \quad (11)$$

The output voltage  $V$ :

$$V = V_{N_1} + V_{b1N_1} = V_{N_2} + V_{b1N_2} = V_{N_3} + V_{b1N_3} \quad (12)$$

$V_{N_i}$ ,  $I_{N_i}$ ,  $V_{b1N_i}$  were voltage, current and blocking diode voltage of the modules corresponding to  $G_i$  respectively. The  $N_i$  ( $i=1,2,3$ ) was substituted into the formula (5), then

$$I_{N_i} = I_{pvi} - I_{01} \left[ \exp\left(\frac{(V - V_{b1N_i}) + R_{Ms} I_{N_i} / N_i}{N_s V_{T1} / N_i}\right) - 1 \right] - I_{02} \left[ \exp\left(\frac{(V - V_{b1N_i}) + R_{Ms} I_{N_i} / N_i}{N_s V_{T2} / N_i}\right) - 1 \right] - \frac{(V - V_{b1N_i}) + R_{Ms} I_{N_i} / N_i}{R_{Mp} / N_i} \quad (13)$$

$$V_{b1N_i} = \frac{AKT}{q} \ln\left(\frac{I_{N_i}}{I_0} + 1\right) \quad (14)$$

(2)  $N_1$  and  $N_2$  modules output power

With the array output voltage increasing, as  $V \in (V_{oc3}, V_{oc2}]$ ,  $G_3$  modules could not continue to provide the output voltage of array. The blocking diodes series with the  $N_3$  modules were in the blocking state under a reverse bias. At this time, the module of  $G_1$  and  $G_2$  output power. Because the light intensity had little effect on the open circuit

voltage of PV module,  $(V_{oc3}, V_{oc2}]$  was a smaller range, in which array power output decreased rapidly. The output characteristics equations of I-V showed:

$$I = I_{N_1} + I_{N_2} \quad (14)$$

$$V = V_{N_1} + V_{b1N_1} = V_{N_2} + V_{b1N_2} \quad (15)$$

### (3) N1 modules output power

when the output voltage of array increased to  $V \in (V_{oc2}, V_{oc3}]$ , only G1 modules output power. The output characteristics equations were:

$$I = I_{N_1} \quad (16)$$

$$V = V_{N_1} + V_{b1N_1} \quad (17)$$

To sum up, in a non-uniform illumination, as output voltage  $V \in (V_{oc3}, V_{oc2}]$ , the output power increased with the voltage increasing and the power peak point appeared. The output current and power reduced with continuing to increase the output voltage. As  $V$  in the intervals  $(V_{oc3}, V_{oc2}]$  and  $(V_{oc2}, V_{oc1}]$ , Current and power continued to decrease, there was a maximum power point on output curve.

### 3.3. Mathematical Models of Series-parallel PV Array

$M \times N$  PV series-parallel array consisted of  $M$  series modules in parallel and each series array contained  $N$  PV modules. The topology structure was shown in Figure 4.

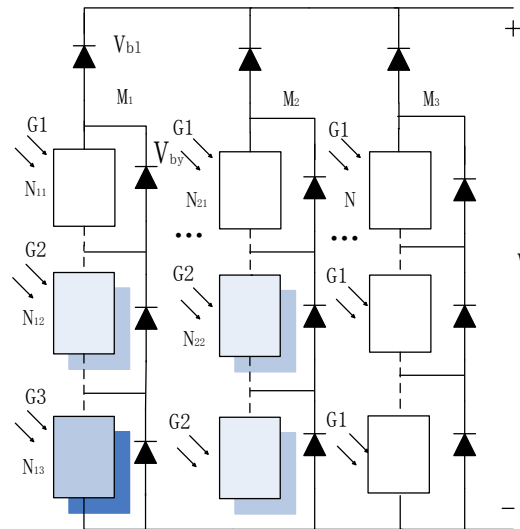


**Figure 4. Series-Parallel PV Array**

In Figure 4,  $N_{11}(G1)$ ,  $N_{12}(G2)$ ,  $N_{13}(G3)$ ,  $N_{11} + N_{12} + N_{13} = N$  were in the  $M_1$  series branch;  $N_{21}(G1), N_{22}(G2), N_{21} + N_{22} = N$  in the  $M_2$ ;  $N$  modules for  $G1$  in  $M_3$ , and  $M_1 + M_2 + M_3 = M$ . The array output voltage was divided into three intervals for the voltage as a reference,  $[0, N_{11}V_{oc1} + N_{12}V_{oc2} + N_{13}V_{oc3}]$ ,  $(N_{11}V_{oc1} + N_{12}V_{oc2} + N_{13}V_{oc3}, N_{21}V_{oc1} + N_{22}V_{oc2}]$  and  $(N_{21}V_{oc1} + N_{22}V_{oc2}, NV_{oc1}]$ .

### 3.3.1 M Parallel Branches Output Power

As the output voltage  $V \in [0, N_{11}V_{oc1} + N_{12}V_{oc2} + N_{13}V_{oc3}]$ , M branches output voltage V. Current I was the sum of M branches current.

$$V = V_{M_1} + V_{blM_1} = V_{M_2} + V_{blM_2} = V_{M_3} + V_{blM_3} \quad (18)$$

$$I = M_1 I_{M_1} + M_2 I_{M_2} + M_3 I_{M_3} \quad (19)$$

$V_{M_i}$  and  $I_{M_i}$  were the output voltage and current of  $M_i$  series branch circuit. The output voltage was determined by the minimum voltage values in each branch.

#### (1) Group M1 series branch analysis

The current was divided into three sections  $[0, I_{cs3}]$ ,  $(I_{cs3}, I_{cs2}]$  and  $(I_{cs2}, I_{cs1}]$  for three illumination levels of the branch. The expression of piecewise function was :

$$V = V_{M_1} + V_{blM_1} = V_{N_{11}} + V_{N_{12}} + V_{N_{13}} + V_{blM_1} \quad 0 \leq I_{M_1} \leq I_{cs3} \quad (20)$$

$$V = V_{M_1} + V_{blM_1} + N_{13}V_{by} = V_{N_{11}} + V_{N_{12}} + V_{blM_1} + N_{13}V_{by} \quad I_{cs3} < I_{M_1} \leq I_{cs2} \quad (21)$$

$$V = V_{M_1} + V_{blM_1} + N_{12}V_{by} + N_{13}V_{by} = V_{N_{11}} + V_{blM_1} + N_{12}V_{by} + N_{13}V_{by} \quad I_{cs2} < I_{M_1} \leq I_{cs1} \quad (22)$$

$V_{N_{11}}$ ,  $V_{N_{12}}$  and  $V_{N_{13}}$  represented the output voltage of  $N_{11}$  (G1),  $N_{12}$  (G2) and  $N_{13}$  (G3).

$$V_{N_{1i}} = N_{1i} R_{Mp} \left\{ I_{pvj} - I_{01} \left[ \exp\left(\frac{V_{N_{1i}} + R_{Ms} I_{M_1} N_{1i}}{N_s V_{T1} N_{1i}}\right) - 1 \right] - I_{02} \left[ \exp\left(\frac{V_{N_{1i}} + R_{Ms} I_{M_1} N_{1i}}{N_s N_{1i} V_{T2}}\right) - 1 \right] - I_{M_1} \right\} - R_{Ms} I_{M_1} N_{1i} \quad (i=1,2,3) \quad (23)$$

$$V_{blM_1} = \frac{AKT}{q} \ln\left(\frac{I_{M_1}}{I_0} + 1\right) \quad (24)$$

$$V_{by} = \frac{AKT}{q} \ln\left(\frac{I_{M_1}}{I_0} + 1\right) \quad (25)$$

#### (2) Group M2 series branch analysis

The output voltage of M2 and M3 branches was equal to M1. That was

$$V = V_{M_2} + V_{blM_2} = V_{N_{21}} + V_{N_{22}} + V_{blM_2} \quad (26)$$

$V_{N_{21}}$  and  $V_{N_{22}}$  represented the output voltage of  $N_{21}$  (G1) and  $N_{22}$  (G2).

$$V_{N_{2j}} = N_{2j} R_{Mp} \left\{ I_{pvj} - I_{01} \left[ \exp\left(\frac{V_{N_{2j}} + R_{Ms} I_{M_2} N_{2j}}{N_s V_{T1} N_{2j}}\right) - 1 \right] - I_{02} \left[ \exp\left(\frac{V_{N_{2j}} + R_{Ms} I_{M_2} N_{2j}}{N_s N_{2j} V_{T2}}\right) - 1 \right] - I_{M_2} \right\} - R_{Ms} I_{M_2} N_{2j} \quad (j=1,2) \quad (27)$$

$$V_{blM_2} = \frac{AKT}{q} \ln\left(\frac{I_{M_2}}{I_0} + 1\right) \quad (28)$$

#### (3) Group M3 series branch analysis

M3 series branch could be regarded as the array of  $M3 \times N$  only with G1 illumination. The output voltage V could be expressed as  $V = V_{M_3} + V_{blM_3} = V_N + V_{blM_3}$

$V_N$  indicated the output voltage of  $M3 \times N$  array.



Take the  $M3 \times N$  into the formula (6) that the output current could be obtained.

$$I_{M_3} = I_{pv1} - I_{01} \left[ \exp\left(\frac{V_N + R_{M_3} I_{M_3} (N/M_3)}{N_s V_{T1}}\right) - 1 \right] - I_{02} \left[ \exp\left(\frac{V_N + R_{M_3} I_{M_3} (N/M_3)}{N_s V_{T2}}\right) - 1 \right] - \frac{V_N + R_{M_3} I_{M_3} (N/M_3)}{R_{Mp} (N/M_3)} \quad (29)$$

**3.3.2. M2 and M3 Branches Output Power:** When the output voltage of PV array worked in the  $(N_{11}V_{oc1} + N_{12}V_{oc2} + N_{13}V_{oc3}, N_{21}V_{oc1} + N_{22}V_{oc2})$ , M1 series branch could not continue to provide the output voltage of the PV array, at the same time M2 and M3 output power commonly.

$$V = V_{M_2} + V_{blM_2} = V_{M_3} + V_{blM_3} \quad (30)$$

$$I = M_2 I_{M_2} + M_3 I_{M_3} \quad (31)$$

$V_{M_2}$ ,  $V_{M_3}$  and  $I_{M_2}$ ,  $I_{M_3}$  were the output voltage and current of M2 and M3.

#### (1) M2 series branch analysis

The output current was divided into two sections  $[0, I_{cs2}]$  and  $(I_{cs2}, I_{cs1}]$  for two illumination level in M2 series branch. The expression of piecewise function was as follows:

$$V = V_{M_2} + V_{blM_2} = V_{N_{21}} + V_{N_{22}} + V_{blM_2} \quad 0 \leq I_{M_2} \leq I_{cs2} \quad (32)$$

$$V = V_{M_2} + V_{blM_2} + N_{22}V_{by} = V_{N_{21}} + V_{blM_2} + N_{22}V_{by} \quad I_{cs2} < I_{M_2} \leq I_{cs1} \quad (33)$$

#### (2) M3 series branch analysis

M3 series branch voltage was equal to the voltage of M2.

$$V = V_{M_3} + V_{blM_3} = V_N + V_{blM_3} \quad (34)$$

**3.3.3. M3 Series Branch Analysis:** When the output voltage of array worked in  $(N_{21}V_{oc1} + N_{22}V_{oc2}, NV_{oc1})$ , M1 and M2 could not satisfy the output voltage of the PV array so that only M3 could output power. The expressions of output voltage V and current I were:

$$V = V_{M_3} + V_{blM_3} = V_N + V_{blM_3} \quad (35)$$

$$I = I_{pv1} - I_{01} \left[ \exp\left(\frac{V_N + R_{M_3} I (N/M_3)}{N_s V_{T1}}\right) - 1 \right] - I_{02} \left[ \exp\left(\frac{V_N + R_{M_3} I (N/M_3)}{N_s V_{T2}}\right) - 1 \right] - \frac{V_N + R_{M_3} I (N/M_3)}{R_{Mp} (N/M_3)} \quad (36)$$

From the above mathematical model of  $M \times N$  series-parallel array, the output power was the numerical superposition corresponding output voltage. Because there were multiple unknown variables in the output expression of the PV array, the peak power point order of array was related with the illumination level of the three series array. At the same time, the distribution voltage range was very small.

## 4. The Simulation and Experimental Analysis

Taking KG200GTPV module in table1 as an example, the simulation experiment was carried out through the MATLAB programming m file by use of the parameters in Table 2.

#### 4.1. Series PV Array Simulation

The topology of four series PV array and light distribution was shown in table 3. The temperature and light intensity was assumed respectively 25°C and  $G1=1000W/m^2$ ,  $G2=600W/m^2$  and  $G3=400W/m^2$ .

**Table 3. Topology of Series PV arrays and Light Distribution**

type	series modules	G1 modules	G2 modules	G3 modules
A	30	30	0	0
B	30	10	10	10
C	30	20	5	5
D	30	5	5	20

The output current range took the short circuit current under different illuminations as the endpoint, that were  $I_{cs1}=8.2279A$ ,  $I_{cs2}=4.93674A$ ,  $I_{cs3}=2.46837A$ .

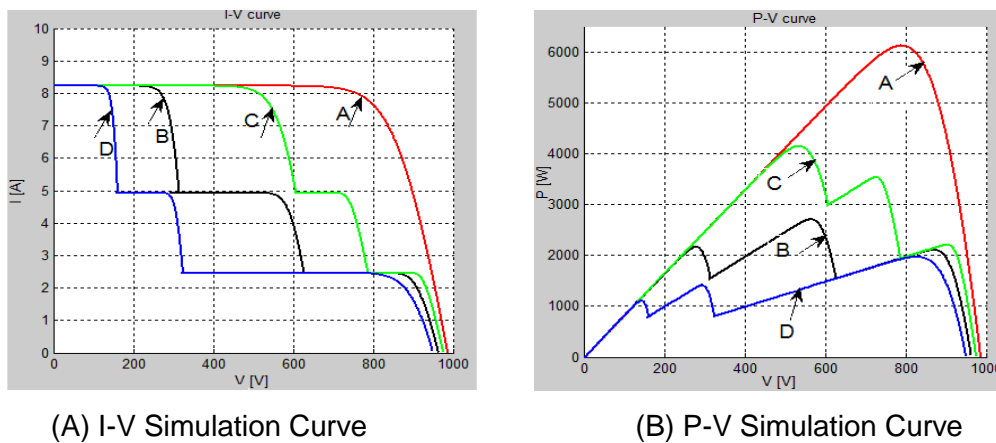


**Figure 5. Simulation Curve of Series PV Array**

Figure 5 (a) and (b) showed the simulation curves I-V and P-V of four different types series arrays. The output curve was shown as curves under uniform illumination environment (type A) and the output had a single peak. There were three power peak points in the curve under the non-uniform illumination and the maximum output power dropped significantly. PV array generated photocurrent different photocurrents caused by different illumination. When the output current was larger than that of model photocurrents the module voltage became negative. The bypass diodes were in conduction state which generated different turning point at different illumination.

So, the number of power peak point and the current ladder was the same as the levels of illumination received. The maximum power point ( $V, P$ ) of A, B, C and D global are respectively (789.69V, 6138.7W), (569.47V, 2710.5W), (534.49V, 4147.9W) and (842.63V, 1969.9W). It could be concluded by the type of C, B, D curves that the global peak position was related with the numbers of module with maximum illumination, the more the maximum illumination numbers were peak points appeared earlier.

#### 4.2. Parallel PV Array Simulation

The structure of parallel PV arrays and light distribution was shown as Table 4.

**Table 4. Structure of Parallel PV Arrays and Light Distribution**

type	Parallel modules	G1 modules	G2 modules	G3 modules
A	30	30	0	0
B	30	10	10	10
C	30	20	5	5
D	30	5	5	20

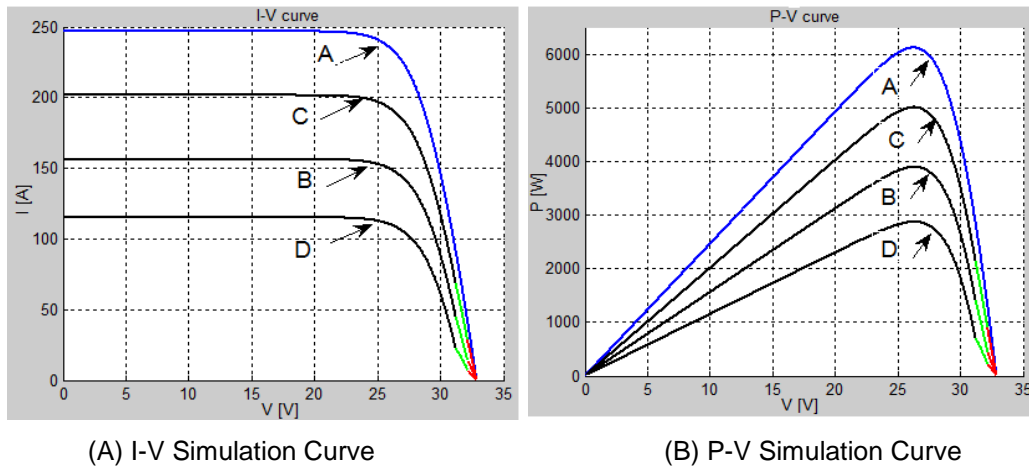


**Figure 6. Simulation Curve of Series Parallel Array**

Figure 6 showed the I-V and P-V simulation curves of parallel PV array. The curves (B, C, D) under non-uniform illumination changed slightly compared with the curve (A) under uniform illumination. The output voltage range was divided with the endpoint of the maximum open circuit voltage, that were  $V_{oc1} = 32.9030V$ ,  $V_{oc2} = 32.1943V$ ,  $V_{oc3} = 31.2326V$ . The global maximum power point (V,P) of curve A, B, C and D respectively were (26.3303V,6167.3W), (26.5726V,3943.7), (26.4113 V,5027.4 W) and (26.5727 V,2898.4W).

The peak point voltage of B, C, D P-V curve was obviously close to curve A and all the maximum power points located in the first section curve. The maximum output power change sharply with the array illumination. Three voltage intervals  $[0, V_{oc3}]$ ,  $(V_{oc3}, V_{oc2}]$ ,  $(V_{oc2}, V_{oc1}]$  were corresponding to black, green and red segments in B, C, D curves. The output voltage appeared different turning points in different illumination due to the series of the blocking diodes. Therefore, the turning points of power and current curves were equal to that of illumination levels.

In uniform illumination, the maximum output power of series array (Pms) was 6138.7W and 6167.3W (Pmp) in the parallel array, and they were almost same. However, the output power of the parallel module was respectively 1.45, 1.21 and 1.47 times that of series modules under non-uniform illumination. The power output of parallel array increased significantly, and the output characteristics of P-V were simple and easier to track the MPPT. So the parallel array had the higher generating efficiency. Parallel photovoltaic array should be considered priority to in the selection of topology structure in small photovoltaic power system.

### 4.3. Series-Parallel PV Array Simulation

Series-parallel PV array consisted of 30 photovoltaic modules connected in parallel, each of the 10 modules in series to form a branch. The topological structure and light distribution was shown in Table 5.

**Table 5. Structure of Series Parallel PV Array and Light Distribution**

type	branch	G1 modules	G2 modules	G3 modules
A	I	10	0	0
	II	10	0	0
	III	10	0	0
B	I	10	0	0
	II	0	10	0
	III	0	0	10
C	I	4	3	3
	II	4	3	3
	III	4	3	3
D	I	2	3	5
	II	0	10	0
	III	10	0	0

Simulation curve Figures 7 was plotted according to four type of non-uniform illumination.

Type A: Uniform illumination for each branch G1, the curve was shown as A (black) in Figure 9.

Type B: The illumination of three branches were  $G1=1000\text{W/m}^2$ ,  $G2=600\text{ W/m}^2$ ,  $G3=300\text{W/m}^2$ , with voltage ranges  $[0, V_{oc3}]$ ,  $(V_{oc3}, V_{oc2}]$ ,  $(V_{oc2}, V_{oc1}]$  corresponding to blue, green and red segments in curve B.

Type C: Each branch with the same illumination had 4(G1), 3(G2) and 3(G3) models. The current was divided into three sections  $[0, I_{cs3}]$ ,  $(I_{cs3}, I_{cs2}]$  and  $(I_{cs2}, I_{cs1}]$  in each branch, which corresponded to the red, green and blue segments in curve C.

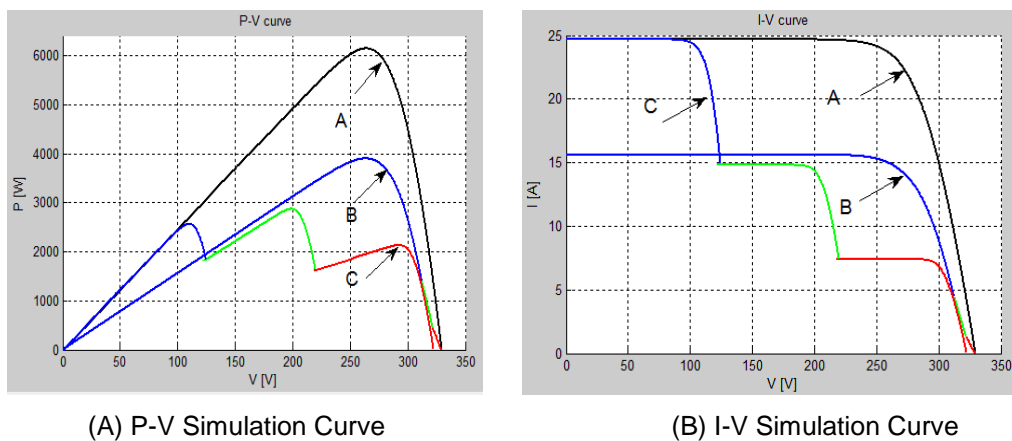


**Figure 7. Simulation Curve of Series Parallel PV Array**

Type D: There were 2(G1), 3(G2), 5(G3) models in the first branch, and all the modules (10) for G2 and G3 in II and III branch. The voltage ranges for the array was  $[0, 2V_{oc1}+3V_{oc2}+5V_{oc3}]$ ,  $(2V_{oc1}+3V_{oc2}+5V_{oc3}, 10V_{oc2}]$ ,  $(10V_{oc2}, 10V_{oc1}]$ . All the 10, 2 (G1), and 3 (G2), 2 (G1) modules output power sequentially. According to the same output voltage for each branch, the current of II and III branches was calculated from the I branch. The curves of I (blue), II (red) and III (green) were plotted in Figure 8, then the array output

power was calculated and plotted in curve D (cyan). As the output voltage in ( $2V_{oc1}+3V_{oc2}+5V_{oc3}, 10V_{oc2}$ ], I branch didn't output power external. The output power of the array could be calculated from the current in II and III branch. The curves were plotted II (green) and III (red).

As the output voltage in ( $10V_{oc2}, 10V_{oc1}$ ], I and II branches didn't output power external. The curve of III was showed in black.

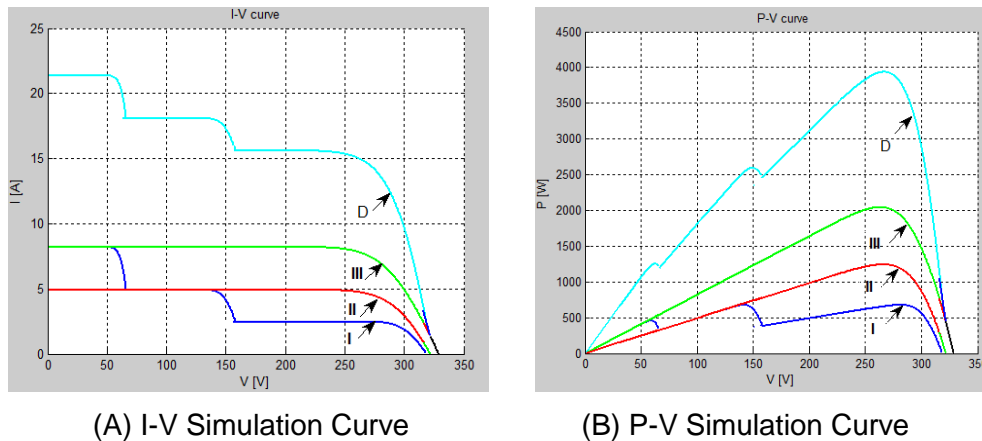


**Figure 8. Simulation Amplification Curve of Series Parallel PV Array**

As could be seen from Figure 8, the output characteristic of series-parallel array was more complex under non-uniform illumination. Curve D was the physical superposition of I, II and III and exhibited series characteristic within current range, and the curve shape was close to curve I. Curve D exhibited parallel characteristic within voltage range and was consisted three curves in three voltage ranges. The peak power point was at the first voltage range.

## 5. Conclusions

The following conclusions were as follows by the theoretical analysis and simulation experiments.

(1) The curve of output power was multi-peak (multi-line) for the existence of bypass diodes and blocking diode in the array and the mathematical model was piecewise functions

(2) In series array, the illumination level determined the number of power peak point and illumination distribution determined distribution of the peak point and the peak voltage.

(3) The output power was superposition of each module when the model voltages were equal in the parallel array. The output voltage and power was superimposed by the value of maximum output voltage and the corresponding module output power. The output curve shape was closed to that of uniform illumination and had a single peak. The composition of the line was determined by the number of illumination levels. It had higher power generation efficiency than the serial array under the same conditions.

(4) There were multiple peak power points in the output power of series-parallel array. The output characteristics of a series-parallel array were not influenced by the number of series branches under the same illumination distribution and it had been with the series arrays feature (such as C in Figure 8). If each series branch had a different illumination level but the same distribution, the branch of maximum illumination level determined the curve shape and maximum output power point position. It had been with the parallel arrays feature. A series-parallel array consisted by different illumination

series branched, which exhibited series features within a certain current range and parallel features within a certain voltage range.

## Acknowledgements

This paper is supported by the Science and technology project of Beijing Municipal Education Commission (NO. KM201310016014) and D funded project to cultivate talents in Beijing City (NO. 2013D005017000008).

## References

- [1] A. Kane and V. Verma, "Characterization of PV cell-environmental factors consideration", International Conference on Power Energy and Control, (2013) Feb 6-8; India.
- [2] M. Abdulkadir, A. Samosir and A. Yatim, "APN Journal of Engineering and Applied Sciences", 7, 617 (2012).
- [3] D. Silva and J. Fernandes, "Solar Energy", 84, 1985(2010).
- [4] M. Seyedmahmoudian and S. Mekhilef, "Energies", 6, 128 (2013).
- [5] Y. Ji and J. Kim. "C-language based PV array simulation technique considering effects of partial shading", IEEE International Conference on Industrial Technology, (2009) Feb10-13; Australia.
- [6] R. Ramaprabha. "MATLAB Based Modelling to Study the Influence of Shading on Series Connected SPVA", Second International Conference on Emerging Trends in Engineering and Technology, (2009) December 16-18; India.
- [7] R. Ramaprabha and B.L. Mathur, "Characteristics of solar PV array under partial shaded conditions", TENCON 2008 - 2008 IEEE Region 10 Conference, (2008) Nov 18-21; USA.
- [8] X. Liu, X. Qi and S. Zheng, "Journal of System Simulation", 24, 1 (2012).
- [9] X. Liu, X. Qi and S. Zheng, 34, 1 (2010).
- [10] T. Jung and J. Ko, "Solar Energy", 92, 214 (2013).
- [11] J. Zhang, X. Wei and Z. Hui, "Advanced Materials Research", 834, 1145 (2014).
- [12] H. Patel and V. Agarwal, "IEEE transactions on energy conversion", 23, 1 (2008).
- [13] K. Ishaque, Z. Salam and H. Taheri, "Journal of Power Electronics", 11, 1(2011).
- [14] D. Alberto and C.L. George, "Energy", 55, 466 (2013).
- [15] R. Carlos, R. Sánchez and H. Diego, "Applied Energy", 103, 278 (2013).
- [16] M.C. Alonso-Garcı, "Renewable Energy", 31, 1986 (2006).
- [17] Yan and J. Li, "Machine Building Automation", 40,123(2011).